# Exponential energy growth in a Fermi accelerator

Kushal Shah[*]

*Faculty of Mathematics and Computer Science, Weizmann Institute of Science, P.O. Box 26, Rehovot 76100, Israel*

Dmitry Turaev[†]

*Department of Mathematics, Imperial College London, London SW7 2AZ, United Kingdom*

Vered Rom-Kedar[‡]

*The Estrin Family Chair of Computer Science and Applied Mathematics, Weizmann Institute of Science, P.O. Box 26, Rehovot 76100, Israel*

An unbounded energy growth of particles bouncing off two-dimensional (2D) smoothly oscillating polygons is observed. Notably, such billiards have zero Lyapunov exponents in the static case. For a special 2D polygon geometry—a rectangle with a vertically oscillating horizontal bar—we show that this energy growth is not only unbounded but also exponential in time. For the energy averaged over an ensemble of initial conditions, we derive an *a priori* expression for the rate of the exponential growth as a function of the geometry and the ensemble type. We demonstrate numerically that the ensemble averaged energy indeed grows exponentially, at a close to the analytically predicted rate—namely, the process is controllable.

PACS number(s): 05.45.−a, 29.20.−c

## I. INTRODUCTION

The problem of Fermi acceleration has attracted a significant interest of researchers since 1949. It was originally proposed by Fermi [1] and later refined by Ulam [2] to explain the acceleration of cosmic rays observed by Hess [3]. The Fermi-Ulam model [4,5] consists of a particle bouncing between two rigid walls, one of which is fixed and the other oscillates periodically. It is now well established that for the one-dimensional Fermi-Ulam model, the particle cannot gain energy unboundedly if the wall motion is smooth. However, it has been shown that unbounded energy growth can be achieved when the particle motion takes place in the presence of potentials [6,7] or if one introduces a relativistic factor in the equations of motion [8]. Nonsmooth motion and stochastic fluctuations may also lead to unbounded energy growth [9] which is typically polynomial in time [10].

More recently, it was suggested that chaotic two-dimensional billiards may provide the needed randomness for the acceleration under smooth oscillations [11–16]. The quantum mechanical oscillating chaotic billiards also play an important role in the modeling of mesoscopic devices [17]. It has been conjectured [13] and proven [16] that a sufficient condition for unbounded energy growth in two-dimensional billiards with oscillating boundaries is the chaotic nature (i.e., the existence of positive Lyapunov exponents on a nontrivial set) of the underlying static billiard. The existence of orbits of linear energy growth was established for the so-called Mather problem in [18–21]. Finally, it was numerically shown that there can be a very slow unbounded energy growth even when the static billiard is integrable—such a

growth was observed in oscillating elliptical billiards [22].

Here, we consider polygonal billiards. While polygonal billiards have zero Lyapunov exponents, almost all of them are nonintegrable [23]. The return map to a section in such billiards may be sometimes related to interval exchange maps [24], so one may suspect that a smooth oscillation of a boundary component is "ideologically" equivalent to a nonsmooth oscillation of a one-dimensional accelerator. Indeed, for many polygonal geometries, when the oscillation amplitude is small enough, we observe an unbounded energy growth at a linear rate (as a function of the number of collisions [25]), which is similar to the nonsmooth one-dimensional case [10] and to the strongly chaotic smooth case [13] [see, e.g., Fig. 2(b)]. Thus, we conjecture that pseudointegrability [26] is a sufficient condition for achieving unbounded energy growth in billiards with smoothly oscillating boundaries.

May a faster rate of energy growth be achieved? In [16], a mechanism was proposed for achieving an exponential energy growth in chaotic billiards (those with a nontrivial hyperbolic invariant set) which are subjected to slow boundary oscillations. Namely, it was shown that when two (or more) hyperbolic periodic orbits change their lengths in a nonsynchronous fashion, a particle that visits their neighborhoods in the correct order will experience exponential energy growth, and the hyperbolicity of the chaotic set was then used to establish that such synchronized visits may indeed be arranged by specific orbits. Exactly the same effect one should encounter for a geodesic flow on a surface with negative curvature when the curvature is slowly changing with time, see [21]. However, as indicated in [16], most orbits will experience only quadratic in time energy growth: as the velocity of the particle inside the breathing billiard increases, the jumps between different hyperbolic periodic orbits start to happen, for a typical orbit, too fast; this leads to an effective averaging of the energy increments or decrements, which

[*]kushal.shah@weizmann.ac.il

[†]d.turaev@imperial.ac.uk
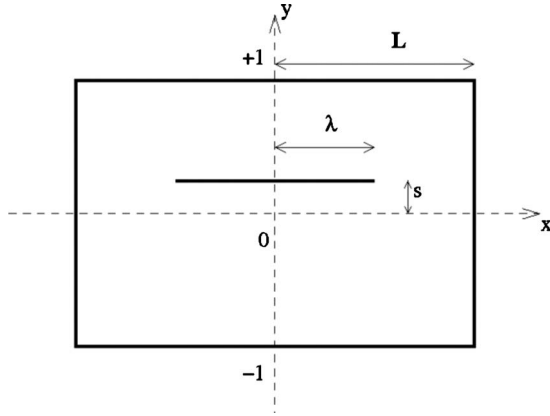
[‡]vered.rom-kedar@weizmann.ac.il

FIG. 1. Geometry of the slitted rectangle. Hereafter, unless otherwise noted, we consider the rectangular billiard with an oscillating bar with: $L=2$, $\lambda=1$, $f(t)=-0.1\cos(\frac{2\pi}{70}t)$.

does not impede the energy growth completely, yet slows it down significantly.

Inspired by this analysis, we design a simple polygonal billiard that has two families of periodic orbits that change their lengths in an antisynchronous way: a rectangle with an oscillating bar inside. The static version was previously introduced in [27,28], and was used to study weak mixing along filamented surfaces in [29]. We show that the slow bar oscillations inside this billiard lead to exponential energy growth on average, i.e., it is much faster than any previously known configuration.

Below, we explain the setting of the problem and calculate analytically the exponential gain or loss of energy a particle experiences when it completes one pass along the oscillating bar. We then argue that for fast particles the locations above or below the bar may be viewed as a sequence of independent random variables, and that this random process is in favor of gaining energy. Indeed Eqs. (6) and (7) show that the expected value of the energy gain factor after one revolution of the particle across the box is, typically, greater than 1. Numerically, we verify that generic ensembles of initial conditions do exhibit exponential energy growth, with the numerically observed rate quite well agreeing with the analytic predictions.

## II. SLITTED RECTANGLE

Consider a billiard in a rectangle with a bar as shown in Fig. 1 (see [27–29]). By symmetry, we may consider half of the slitted rectangle: $R_s=\{(x,y)\,|\,(y\in[-1,1],x\in[0,L])\backslash (y=s,x\in[0,\lambda])\}$, where $s\in(-1,1)$ indicates the slit vertical position. To achieve acceleration, let the slit oscillate slowly: $s=f(\theta)=\bar{f}+\tilde{f}(\theta)$, $\theta\in[0,2\pi]$, $\theta=\omega t$, where $\langle\tilde{f}(\theta)\rangle=0$. The slit vertical velocity is $V(t)=\dot{s}=\omega f'(\theta)$. The phase space variables for this billiard geometry are $(t_n,x_n,y_n,u_n,v_n)$, where $t_n$ is the time instant of the $n$th collision, $\theta_n=\omega t_n$ is the phase of the slit at the collision time, $(x_n,y_n)$ is the location of the particle at $t_n$, and $(u_n,v_n)$ is the velocity vector of the particle immediately after the $n$th collision. The particle undergoes elastic collisions from all the boundaries. Crucially, the hori-

zontal speed $u=|u_n|$ remains a constant of motion, whereas the vertical speed changes only when the moving slit is met:

$$v_{n+1}=2\omega f'_n-v_n \quad \text{when}\{y_n=f_n,x_n\in[0,\lambda]\}, \quad (1)$$

where $f_n=f(\theta_n)$ and $f'_n=f'(\theta_n)$.

Since the horizontal speed stays constant, the time the particle spends oscillating above or below the slit (at $x\in[0,\lambda]$) is simply $T_\lambda=2\lambda/u$, and the time to return to a vertical section after completing one cycle around the rectangle is $T_L=2L/u$. Hence, the phase shift of the slit after time $T_\lambda$ is $\theta_\lambda=2\omega\lambda/u$ and the phase shift of the slit after a full revolution of the particle is $\theta_L=2\omega L/u$.

During the slit-travel time the particle's vertical speed is changing according to

$$v_{n+1}=v_{n-1}+2\omega f'_{n+1}, \quad (2)$$

where

$$t_{n+1}=\begin{cases} t_{n-1}+\dfrac{2-f_{n-1}-f_{n+1}}{v_{n-1}} & \text{motion above the slit} \\[2mm] t_{n-1}-\dfrac{2+f_{n-1}+f_{n+1}}{v_{n-1}} & \text{motion below the slit.} \end{cases}$$

$$(3)$$

For sufficiently fast particles $(t_{n+1}-t_{n-1})\to 0$. Thus, we may approximate these difference equations by the ODEs

$$\frac{dv}{dt}=\begin{cases} \omega v\,\dfrac{f'(\theta)}{1-f(\theta)} & \text{motion above the slit} \\[2mm] -\omega v\,\dfrac{f'(\theta)}{1+f(\theta)} & \text{motion below the slit.} \end{cases} \quad (4)$$

Integrating from the entry phase $\theta$ up to the exit phase $\theta+\theta_\lambda$, the exit velocity $\bar{v}$ may be found:

$$\frac{\bar{v}}{v}=\begin{cases} \dfrac{1-f(\theta)}{1-f(\theta+\theta_\lambda)} & \text{motion above the slit} \\[2mm] \dfrac{1+f(\theta)}{1+f(\theta+\theta_\lambda)} & \text{motion below the slit.} \end{cases} \quad (5)$$

Depending on the values of $\theta$ and $\theta_\lambda$ and on whether the particle goes above the bar or below it in each cycle, the particle will either gain or loose the kinetic energy at each passing of the slit.

The values of $(\theta,\theta_\lambda)$ are determined by the particles' horizontal velocity. The phase gained when the particle traverses the slit is $\theta_\lambda=2\lambda\omega/u$. The distribution of $\theta$, the slit phase when the trajectory enters the slit, depends on $\theta_L$: if $\theta_L/\pi$ is rational, then $\theta(\text{mod }2\pi)$ takes only a finite number of values, otherwise it densely covers $[0,2\pi]$. We should emphasize again that the dynamics in $\theta$ is completely regular as the horizontal velocity is preserved.

Next, we argue that in the regime where the vertical velocity is large and growing, the vertical location of the particle after several rounds is essentially unpredictable: it depends sensitively on the exact exit point and velocity at the previous iterate. To explain the effect, let us consider in more details the derivation of Eq. (5). In this equation the entry phase $\theta$ represents the phase of the slit at the time of the first

collision of the particle with the bar. Thus, two close-by initial conditions that are $\delta y$ apart and hit the bar from the same side produce a phase shift $\delta\theta = \omega\delta y/v$. Now, $\partial\bar{v}/\partial\theta$ is proportional to $v$ [see Eq. (5), cancellations are possible, but occur only at specific $(\theta, \theta_\lambda)$ values]. Hence, two initial conditions that enter the upper part of the slit with the same velocity and slightly different vertical positions, $y$ and $y + \delta y$, will exit with vertical velocities that are $\delta\bar{v} \propto \delta y$ apart. If the energy grows exponentially, this small difference will magnify exponentially and thus the difference between the return vertical positions will also diverge exponentially. This means that even though the sequence of up and down splits is deterministic, the correlations decay fast with time.

Thus, we hereafter employ, as a modeling hypothesis, the view that the particle motion is a random process, with the particle up and down positions being independent random variables. Namely, we assume that the probability to fall into the upper part at the entry phase $\theta$ is proportional to the normalized $y$-interval length, $[1 - f(\theta)]/2$, and is independent of the history of the previous rounds. Then, $\mu$, the expected value of gain in the kinetic energy in one cycle around the rectangle, for a single particle trajectory that enters the slit with the phase $\theta$ and horizontal velocity $u$ is estimated as

$$\mu_\theta = \mathbb{E}[\bar{v}^2/v^2] = \frac{1-f(\theta)}{2}\left(\frac{1-f(\theta)}{1-g(\theta)}\right)^2 + \frac{1+f(\theta)}{2}\left(\frac{1+f(\theta)}{1+g(\theta)}\right)^2, \tag{6}$$

where $g(\theta) := f(\theta + \theta_\lambda)$. It is easy to check that the right-hand side has, as a function of $g$, a minimum at $g = f$ (there $\mu_\theta = 1$), which means that

$$\mu_\theta > 1 \quad \text{if} \quad f(\theta) \neq f(\theta + \theta_\lambda). \tag{7}$$

Realizing that the process of energy gain is multiplicative, we further notice, by a similar computation, that the expectation value of the logarithmic gain is also positive,

$$m_\theta = \mathbb{E}[\ln(\bar{v}^2/v^2)]$$

$$= [1 - f(\theta)]\ln\frac{1-f(\theta)}{1-g(\theta)} + [1 + f(\theta)]\ln\frac{1+f(\theta)}{1+g(\theta)}$$

$$> 0, \quad \text{if} \quad f(\theta) \neq f(\theta + \theta_\lambda). \tag{8}$$

Equation (7) obviously implies an exponential energy growth for the expected value of the particle's energy, whereas Eq. (8) also implies that almost every initial condition produces exponentially accelerating trajectory (see below).

In order to estimate the ensemble growth rate $R_{\theta_\lambda}$, consider the energy gain after each cycle around the rectangle as a random variable, $X_\theta = \bar{v}^2/v^2$, so the energy gain after $N$ cycles is given by

$$R_{\theta_\lambda} := \lim_{t\to\infty} \frac{1}{t}\ln\mathbb{E}\left[\frac{v^2(t)}{v^2(0)}\right], \tag{9}$$

consider the energy gain after each cycle around the rectangle as a random variable, $X_\theta = \bar{v}^2/v^2$, so the energy gain after $N$ cycles is given by

$$\frac{v^2(t = NT_L)}{v^2(0)} = X_{\theta_1}X_{\theta_2}\cdots X_{\theta_N}. \tag{10}$$

We assume that $v$ is sufficiently large so the $\{X_{\theta_i}\}$ may be viewed as independent random variables, with the mean

value of $X_\theta$ given by Eq. (6). This allows the expected value of the product in Eq. (10) to be evaluated as

$$\mathbb{E}\left[\frac{v^2(NT_L)}{v^2(0)}\right] = \mu_{\theta_1}\mu_{\theta_2}\cdots\mu_{\theta_N}$$

$$= \exp\left[\sum_{i=1}^{N}\ln\mu_{\theta_i}\right] = \exp\left[\frac{N}{2\pi}\int_0^{2\pi}\ln\mu_\theta d\theta\right], \tag{11}$$

where the last equality holds only in the nonresonant case, assuming that $\theta_i$ are distributed uniformly over $[0, 2\pi]$ (see Fig. 5 for a resonant case). Notably, while the above formula does not supply information for the energy growth of a single trajectory, it shows that for a finite ensemble of $K$ initial conditions, the observed average energy growth is

$$\left\langle\frac{v^2(t)}{v^2(0)}\right\rangle = \exp(R_{\theta_\lambda}t) + \mathcal{O}\left(\frac{\sigma}{\sqrt{K}}\right), \tag{12}$$

where $\sigma$ denotes the standard deviation of $v^2(t)/v^2(0)$. As we show below, the standard deviation can also grow exponentially in time, so larger ensembles are needed as time progresses. Note that in Eq. (9), $R_{\theta_\lambda}$ is defined by taking the limit $K \to \infty$ first, and the order of the limit cannot be reversed.

To learn about the behavior of individual trajectories, we use Eq. (8) to establish

$$\mathbb{E}\left[\ln\frac{v^2(NT_L)}{v^2(0)}\right] = m_{\theta_1} + m_{\theta_2} + \cdots + m_{\theta_N}$$

$$= \sum_{i=1}^{N}m_{\theta_i} = \frac{N}{2\pi}\int_0^{2\pi}m_\theta d\theta := M_{\theta_\lambda}t, \tag{13}$$

where, again, the second line holds only in the nonresonant case. By the law of large numbers, it follows that for almost every trajectory

$$\lim_{t\to\infty}\frac{1}{t}\ln\frac{v^2(t)}{v^2(0)} = M_{\theta_\lambda}, \tag{14}$$

namely, for typical trajectories the energy grows exponentially [since $M_{\theta_\lambda} > 0$ for most $(\lambda, L)$ by Eq. (14)]. Assuming that the additive process of Eq. (13) leads to a normal distribution, the ensemble rate of energy growth is related to the individual rate of energy growth by $R_{\theta_\lambda} = M_{\theta_\lambda} + 0.5S_{\theta_\lambda}^2$, where $S_{\theta_\lambda}^2t$ is the variance of $\ln\frac{v^2(NT_L)}{v^2(0)}$ [30]. Notice that $R_{\theta_\lambda}$ may be positive even when $M_{\theta_\lambda}$ is negative: this situation corresponds to cases in which most individual trajectories decelerate yet the ensemble average accelerates. Notably, here we showed that both rates are positive.

Next, we compute these rates when the bar oscillation amplitude is small. Let $\tilde{f}(\theta) = \sum_{k=1}^{\infty}[a_k\sin k\theta + b_k\cos k\theta]$ be the Fourier expansion of $\tilde{f}$. Assuming that $|\tilde{f}| \ll 1 - |\bar{f}|$, for an ensemble of initial conditions with a fixed, generically chosen horizontal velocity $|u| = 2\lambda\omega/\theta_\lambda$, it is easy to obtain from Eqs. (6) and (11) that the rate of the averaged energy growth in Eq. (9) is
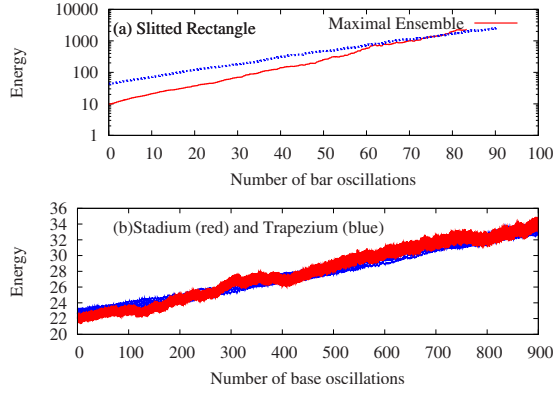
FIG. 2. (Color online) Ensemble averaged energy growth in the slitted rectangle and in a typical pseudointegrable accelerator. All ensembles consist of 1000 randomly placed (uniformly distributed) particles. (a) The rectangle with an oscillating bar produces exponential growth rates that are controlled by the ensemble horizontal velocity. Blue curve: $u_0 = 4\lambda\omega/\sqrt{5}$, $v_0 = 41u_0$ Red curve: $u_0 = 2\lambda\omega/\theta_{max}$, $v_0 = 41u_0$. (b) The oscillating pseudointegrable trapezium (blue/dotted) and the oscillating chaotic half-stadium (red/solid) produce much slower energy growth compared to the rectangle with oscillating bar [notice that the energy axis is logarithmic in (a) and linear in (b)]. The energy growth in the stadium and the trapezium appears to be only linear in time for the first 900 cycles.

$$R_{\theta_\lambda} \approx 3M_{\theta_\lambda} \approx \frac{6\lambda\omega}{L\theta_\lambda(1-\overline{f}^2)} \sum_{k=1}^{\infty} [a_k^2 + b_k^2]\sin^2\frac{k\theta_\lambda}{2} \geq 0.$$

(15)

Similarly, one estimates the standard deviation for the energy gain after $N$ cycles as $\sigma^2[\frac{v^2(t=NT_L)}{v^2(0)}] = \mathbb{E}[X_{\theta_1}^2] \cdot \mathbb{E}[X_{\theta_2}^2] \cdots \mathbb{E}[X_{\theta_N}^2] - \mathbb{E}^2[\frac{v^2(NT_L)}{v^2(0)}]$, which leads, for small $\widetilde{f}$, to

$$\sigma\left[\frac{v^2(t=NT_L)}{v^2(0)}\right] \approx \mathbb{E}\left[\frac{v^2(NT_L)}{v^2(0)}\right]\sqrt{\exp\left(\frac{4R_{\theta_\lambda}t}{3}\right)-1}.$$

(16)

Since the ratio of the standard deviation to the expectation grows exponentially with time, we have to take sufficiently large ensemble sizes in order to ensure that the average energy grows at a rate close to the predicted one.

Figure 2 shows the numerically obtained plot of the averaged energy growth vs time for a random ensemble of initial conditions, comparing three oscillating billiard geometries: the slitted rectangle, a trapezium, and a half-stadium. For small enough oscillation amplitudes, the only geometry which provides exponential energy growth is the slitted rectangle and the observed growth rate matches very well with the predicted rate of Eq. (15). For the one-harmonic case, the rate $R_{\theta_\lambda}$ given by Eq. (15) has a simple decaying oscillatory form, with a global maximum at $\theta_\lambda = \theta_{max}$ where $\theta_{max} = \tan(0.5\theta_{max}) \approx 2.35$, see Fig. 3.

In Fig. 2(a) we present two different ensembles, one with a generic $u$ (blue/dotted curve) and the other with the $u$ that provides maximal growth rate (red/solid curve). A linear fit
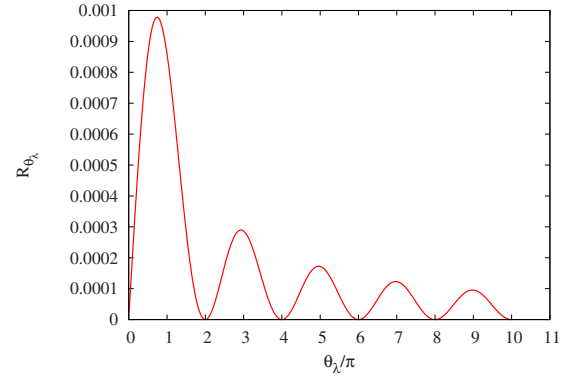


FIG. 3. (Color online) The energy growth rate dependence on $\theta_\lambda$ as predicted by Eq. (15).

to the presented ensembles gives $R_{\theta_\lambda} \approx (6.919 \pm 0.014) \times 10^{-4}$ (blue/dotted) and $R_{\theta_{max}} \approx (9.187 \pm 0.049) \times 10^{-4}$ (red/solid). The corresponding predicted rates are $6.775 \times 10^{-4}$ and $9.755 \times 10^{-4}$. Other ensembles with the same initial velocity or with a distribution of vertical velocities provide a similar energy growth rate. The presented results are computationally solid: the total number of reflections of the particle is less than $5 \times 10^5$ so that the final accumulated numerical error for the ensemble average is smaller than 1.4%. The sample size is sufficient for the presented computational time: taking half the sample size hardly changes the averaged behavior for about 40 bar oscillations, at which the exponential rate is already clearly seen [31]. As can be seen from Eqs. (12) and (16), for an ensemble of $K$ particles, the deviation of the statistical average from the theoretical mean value is $\mathcal{O}(\sigma/\sqrt{K})$, and for a given ensemble size, after long enough time the dispersion effects become important and energy growth is no longer precisely determined by Eq. (9). For the maximal ensemble shown in Fig. 2, after $Q$ oscillations of the bar, we have $\sigma[v^2] \approx \mathbb{E}[v^2]\sqrt{[\exp(0.091Q)-1]/K}$. Thus, the condition, $\sigma[v^2] \ll \mathbb{E}[v^2]$, for the ensemble averaged energy to stay close to the mean in Eq. (9) is satisfied for $Q \ll 11 \ln(K+1)$. For an ensemble of 1000 particles, this implies $Q \ll 75$. As can be seen in Fig. 2(a), the observed energy growth starts deviating from the mean after about 50 oscillations of the bar. On longer time scales, for a fixed ensemble size $K$, we expect that the energy growth rate will converge to the lower value predicted by Eq. (14).

In Fig. 2(b) we present the averaged energy growth of similar ensembles in a typical pseudointegrable oscillating billiard and in an oscillating chaotic billiard. The pseudointegrable billiard is a trapezium with an oscillating base, vertical sides and an inclined top at an angle $\alpha = \pi/18$. The chaotic billiard is a half-stadium with an oscillating base, vertical sides and a half-circle dome. The bottoms' lengths are $2\lambda$ and the billiards are of the same area as the slitted rectangle. We see that both billiards produce a similar averaged energy growth. The averaged energy has an oscillatory component associated with the forcing period and a growing envelope component that appears to be linear in the number of collisions for as long as 900 base oscillations. We have checked that other polygons with an oscillating edge lead to
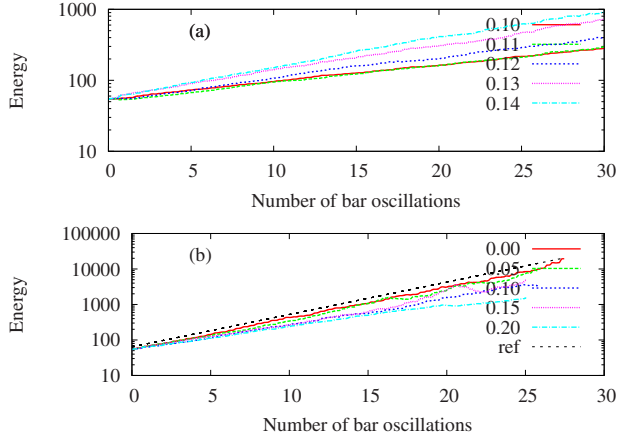
FIG. 4. (Color online) The controllability of the averaged exponential energy growth rate in the slitted rectangle. The energy growth rates for different values of $\langle \tilde{f}^2 \rangle$ and $\bar{f}$ are shown. (a) Dependence on $\langle \tilde{f}^2 \rangle$: Here $f = -a_1 \cos\frac{2\pi}{70}t$, where $a_1 = \{0.10, 0.11, 0.12, 0.13, 0.14\}$, $u_0 = 4\lambda\omega/\sqrt{5}$ and $v_0 = 41u_0$. The exponential energy growth rate increases approximately linearly with $\langle \tilde{f}^2 \rangle$ (as $\langle \tilde{f}^2 \rangle^{1\pm\epsilon}$ where $\epsilon < 0.25$) (b) Dependence on $\bar{f}$: fixing $\frac{\langle \tilde{f}^2 \rangle}{(1-|\bar{f}|)^2}$, and letting $f = \bar{f} - a_1 \cos\frac{2\pi}{70}t$ with $\bar{f} \in [0, 0.2]$ increasing by steps of 0.05, the slope decreases with $\bar{f}$. The dashed line is a straight line that is drawn for reference.

similar linear energy growth rates, which are also typically observed in strongly chaotic, dispersing billiards [it is easy to compute [16] that the rate, linear in the number of collisions, corresponds to a quadratic dependence on time in the long run: as the energy—hence the particle speed—increases, the time interval between collisions decreases; however, the energy growth we observe here is not significant enough to make the nonlinear dependence of the energy on time be visible in Fig. 2(b)].

Next, we show the predictive power of Eqs. (6) and (15) in controlling the averaged exponential growth rate of various ensembles. Using Parseval's theorem, an upper bound for $R_{\theta_\lambda}$ is

$$R_{\theta_\lambda} \leq \frac{12\lambda\omega\langle \tilde{f}^2 \rangle}{L\theta_\lambda(1-\bar{f}^2)} = \frac{12\lambda\omega}{L\theta_\lambda} \frac{\langle \tilde{f}^2 \rangle}{(1-|\bar{f}|)^2} \frac{1-|\bar{f}|}{1+|\bar{f}|} \qquad (17)$$

showing that for a given small oscillation/gap ratio, the best strategy is to keep $\bar{f} = 0$ while increasing $\langle \tilde{f}^2 \rangle$. Figure 4 validates the above formula, demonstrating that we are able to control the exponential growth rate of energy. Figure 4(a) shows that at $\bar{f} = 0$ the exponential growth rate increases with $\langle \tilde{f}^2 \rangle$, whereas Fig. 4(b) shows that for a fixed $\frac{\langle \tilde{f}^2 \rangle}{(1-|\bar{f}|)^2}$, the growth rate decreases with $|\bar{f}|$.

Finally, Fig. 5 shows a resonant ensemble: we take 1000 particles, with $u_0 = 2\lambda\omega/\pi$ so that $\theta_L = 2\pi$ and $\theta_\lambda = \pi$, distributed evenly over $y_0 \in [f(0), 1]$ and fixed $x_0 = 1.01\lambda$ so that $\theta = \theta_0 = 0.005\pi$. Taking sufficiently large $v(0)$ leads to an energy growth rate equal to $(15.92 \pm 0.08) \times 10^{-4}$, namely, larger by a factor of about 1.6 from the maximal averaged rate and by a factor of 1.9 from the averaged growth rate
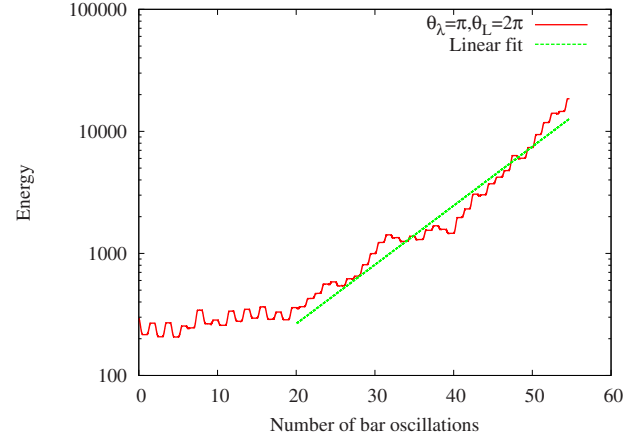


FIG. 5. (Color online) Energy growth rate for a resonant ensemble. The ensemble consists of 1000 particles with $u_0 = 2\lambda\omega/\pi$ and $v_0 = 299u_0$ (so that $\theta_L = 2\pi$ and $\theta_\lambda = \pi$), distributed evenly over $y_0 \in [f(0), 1]$ and fixed $x_0 = 1.01\lambda$ (so that $\theta = \theta_0 = 0.005\pi$). The green line slope provides a growth rate of $(15.92 \pm 0.08) \times 10^{-4}$ whereas the predicted rate is $R = 16.55 \times 10^{-4}$.

predicted by Eq. (15) for $\theta_\lambda = \pi$. The averaged exponential growth here is much noisier than the one we get for generic ensembles—the reason for that is under current study. This much higher growth rate is achieved since the value of $\theta$, the slit phase at the instant of the particle's entrance to the slit region, remains constant for the resonant ensemble. Hence, the averaging of the energy gain over $\theta$ [the last equality in Eq. (11)] should not be applied, and Eq. (6) should be used instead to find the corresponding constant $\mu_\theta$. Our judicial choice of $\theta_0 = 0.005\pi$ near [32] the maximum of $\mu_\theta$ [where, by Eq. (6), $R_{\theta_\lambda} = 16.55 \times 10^{-4}$] allows to obtain a growth rate which is significantly higher than the average.

## III. CONCLUSIONS

We have demonstrated that our Fermi acceleration machine leads to a much faster energy growth than other breathing billiards. Moreover, since we can control the energy growth rate in this accelerator, other issues, such as optimizing the accelerator efficiency by tuning the forcing higher harmonics and the slit averaged position may be now explored.

Would other oscillating billiard geometries lead to an observable averaged exponential growth rate? Though the oscillating stadium has been observed to lead to only quadratic in time energy growth for small oscillation amplitude [13], we have numerically observed that higher oscillation amplitudes can lead to higher growth rates, possibly, yet not surely, exponential. This is under current study.

We now think that the randomization of the particle position and the preservation of the horizontal velocity in the billiard with the interior oscillating bar are both key ingredients in achieving the exponential energy growth for small oscillation amplitudes. Notably, these ingredients keep the process far from statistical equilibrium: one velocity component grows fast, while the other component stays bounded.

Summarizing, we are now able to create exponentially fast acceleration in a smoothly oscillating Fermi accelerator,

and to analytically predict, and thus control, the exponential growth rate that is realized by various ensembles. We believe that this is an exciting discovery that can be perhaps experimentally realized.

[1] E. Fermi, Phys. Rev. **75**, 1169 (1949).

[2] S. M. Ulam, *On Some Statistical Properties of Dynamical Systems*, Proceedings of the 4th Berkeley Symposium Mathematical Statistics Probability, University of California (University of California Press, Berkeley, 1961) Vol. 3, p. 315.

[3] M. Harwit, *Cosmic Discovery: The Search, Scope and Heritage of Astronomy* (The MIT Press, Cambridge, MA, 1984).

[4] M. A. Lieberman and A. J. Lichtenberg, Phys. Rev. A **5**, 1852 (1972).

[5] L. D. Pustyl'nikov, Theor. Math. Phys. **57**, 1035 (1983).

[6] L. D. Pustyl'nikov, Proc. Moscow Math. Soc. **34**, 3 (1977).

[7] D. Dolgopyat, Discrete Contin. Dyn. Syst. **22**, 165 (2008).

[8] L. D. Pustyl'nikov, Theor. Math. Phys. **86**, 82 (1991).

[9] V. Zharnitsky, Nonlinearity **11**, 1481 (1998).

[10] E. D. Leonel and P. V. E. McClintock, J. Phys. A **38**, 823 (2005).

[11] C. Jarzynski, Phys. Rev. E **48**, 4340 (1993).

[12] J. Koiller, R. Markarian, S. O. Kamphorst, and S. P. de Carvalho, Nonlinearity **8**, 983 (1995).

[13] A. Loskutov, A. B. Ryabov, and L. G. Akinshin, J. Phys. A **33**, 7973 (2000).

[14] R. E. de Carvalho, F. C. de Souza, and E. D. Leonel, J. Phys. A **39**, 3561 (2006).

[15] S. O. Kamphorst, E. D. Leonel, and J. K. L. da Silva, J. Phys. A: Math. Theor. **40**, F887 (2007).

[16] V. Gelfreich and D. Turaev, J. Phys. A: Math. Theor. **41**, 212003 (2008).

[17] D. Cohen and D. A. Wisniacki, Phys. Rev. E **67**, 026206 (2003).

[18] S. Bolotin and D. Treschev, Nonlinearity **12**, 365 (1999).

[19] A. Delshams, R. de la Llave, and T. M. Seara, Adv. Math. **202**, 64 (2006).

[20] G. N. Piftankin, Nonlinearity **19**, 2617 (2006).

[21] V. Gelfreich and D. Turaev, Commun. Math. Phys. **283**, 769 (2008).

[22] F. Lenz, F. K. Diakonos, and P. Schmelcher, Phys. Rev. Lett. **100**, 014103 (2008).

[23] E. Gutkin, Physica D **19**, 311 (1986).

[24] M. Keane, Math. Z. **141**, 25 (1975).

[25] As shown in [16] this, in a long run, corresponds to a quadratic growth in time.

[26] P. J. Richens and M. V. Berry, Physica D **2**, 495 (1981).

[27] J. H. Hannay and R. J. McCraw, J. Phys. A **23**, 887 (1990).

[28] H. Masur and J. Smillie, Ann. Math. **134**, 455 (1991).

[29] G. M. Zaslavsky and M. Edelman, Chaos **11**, 295 (2001).

[30] E. L. Crow and K. Shimizu, *Lognormal Distributions: Theory and Applications* (Dekker, New York, 1988).

[31] For example, we obtain a growth rate of $(8.472 \pm 0.058) \times 10^{-4}$, an error of around 0.6% compared to an 0.2% error in the 1000 particle ensemble.

[32] Here, taking the maximizing $\theta_0 = 0$ does not work; since here $f'(0) = g'(0) = 0$, the needed mixing in $y$ is spoiled at $\theta_0 = 0$.